

Monitoring Structure and Valence State of Chromium Sites during Catalyst Formation and Ethylene Oligomerization by in Situ EPR Spectroscopy

Angelika Brückner,^{*,†} Jabor K. Jabor,[†] Ann E. C. McConnell,[‡] and Paul B. Webb[§]

Leibniz-Institut für Katalyse an der Universität Rostock e. V., Branch Berlin, P.O. Box 961156, D-12474 Berlin, Germany, Sasol Technology R&D, 1 Klasie Havenga Road, P.O. Box, 1947 Sasolburg, South Africa, and Sasol Technology UK Ltd, Purdie Building, North Haugh, St. Andrews, FIFE, KY16 9ST, U.K.

Received April 8, 2008

For the first time, a Cr(acac)₃/PNP mixture (PNP = Ph₂PN(*i*-Pr)PPh₂) and a [(PNP)CrCl₂(μ-Cl)]₂ complex were monitored by in situ EPR in cyclohexane and toluene, respectively, during oligomerization of ethylene. For Cr(acac)₃/PNP, Cr³⁺ reduction is faster than low-spin Cr⁺ formation, suggesting that the major active species is EPR-silent, possibly an antiferromagnetic Cr⁺ dimer and/or Cr²⁺. Fast decomposition of [(PNP)CrCl₂(μ-Cl)]₂ to [Cr(η⁶-CH₃C₆H₅)₂]⁺ is a probable reason for low activity.

Introduction

Linear α-olefins such as 1-hexene and 1-octene are important comonomers for the production of polyethylene. Commercially, they are predominantly produced by metal-catalyzed oligomerization of ethylene, which usually leads to a distribution of α-olefins with different chain length that frequently does not match the market demand.¹ Increasing the selectivity of these processes by developing better catalysts is therefore one of the major challenges. A variety of organochromium complexes with different ligands have been developed to catalyze the trimerization of ethylene to 1-hexene with selectivities of up to more than 90%.¹ For the first time, the tetramerization of ethylene to 1-octene has been achieved with up to 70% selectivity also using a Cr-based catalyst system.² The active catalyst was generated in situ by adding modified methyl aluminoxane (MMAO) as activator to a solution of Cr(acac)₃ and a bidentate diphosphinoamine ligand (PNP) in a nonpolar solvent. In the meantime, much higher productivities of 2 to more than 3 million g/g_{Cr} h could be achieved upon systematic optimization of the PNP ligands using different alkyl and cycloalkyl substituents attached to the N atom of the ligand backbone.^{3,4}

Despite extensive previous research, several mechanistic details of ethylene oligomerization on chromium complexes are still a matter of debate.^{5–11} Labeling experiments have provided unequivocal evidence for the operation of a metallacycle mechanism that proceeds via initial oxidative coupling of two

ethylene units and subsequent ethylene insertion into the metallacycle followed by its degradation to liberate alkene.^{11,12} However, the Cr valence state and the sequence of steps involving precatalyst activation are still controversially discussed. For the Cr(acac)₃/PNP/MMAO system, a Cr⁺/Cr³⁺ redox cycle is speculated with dimeric Cr²⁺ intermediates being responsible for the formation of cyclic byproducts.⁵ However, experimental evidence for this assumption has not been provided. The postulation of a Cr⁺/Cr³⁺ redox cycle was derived from the fact that a separately synthesized dimer [(PNP)Cr³⁺Cl₂(μ-Cl)]₂ complex² as well as a separately prepared cationic [(CO)₄Cr⁺(PNP)]⁺ complex¹³ showed good C₈ selectivities, but the nature of the active species existing in solution will of course be different from this precursor. The major role of the aluminoxane activator is generally assumed to be alkylation of the metal followed by alkyl abstraction and formation of an ion pair.^{1,8,13} Recently, it has been demonstrated by DFT calculations that the most probable intermediate forming upon contact of a model PNP-chromacycloheptane complex (PNP = Ph₂PN(*i*-Pr)PPh₂) with methylaluminoxane containing trimethylaluminum, (AlOMe)₃-TMA, and ethylene is an ion pair consisting of a cationic chromacycloheptane complex with coordinated ethylene, [(PNP)Cr(CH₂)₆•C₂H₄]⁺, and a methylated (AlOMe)₃-TMA⁻ anion.⁸ However, it has also been proposed that the activator reduces the metal center in the early

* Corresponding author. Phone: +49 30 6392 4301. Fax: +49 30 6392 4454. E-mail: angelika.brueckner@catalysis.de.

[†] Leibniz-Institut für Katalyse.

[‡] Sasol Technology R&D.

[§] Sasol Technology UK Ltd.

(1) Dixon, J. T.; Green, M. J.; Hess, F. M.; Morgan, D. H. *J. Organomet. Chem.* **2004**, *689*, 3641.

(2) Bollmann, A.; Blann, K.; Dixon, J. T.; Hess, F. M.; Killian, E.; Maumela, H.; McGuinness, D. S.; Morgan, D. H.; Neveling, A.; Otto, S.; Overett, M.; Slawin, A. M. Z.; Wasserscheid, P.; Kuhlmann, S. *J. Am. Chem. Soc.* **2004**, *126*, 14712.

(3) Blann, K.; Bollmann, A.; de Bod, H.; Dixon, J. T.; Killian, E.; Nongodwana, P.; Maumela, M. C.; Maumela, H.; McConnell, A. E.; Morgan, D. H.; Overett, M. J.; Prétorius, M.; Kuhlmann, S.; Wasserscheid, P. *J. Catal.* **2007**, *249*, 244.

(4) Kuhlmann, S.; Blann, K.; Bollmann, A.; Dixon, J. T.; Killian, E.; Maumela, M. C.; Maumela, H.; Morgan, D. H.; Prétorius, M.; Taccardi, N.; Wasserscheid, P. *J. Catal.* **2007**, *245*, 279.

(5) Overett, M. J.; Blann, K.; Bollmann, A.; Dixon, J. T.; Haasbroek, D.; Killian, E.; Maumela, H.; McGuinness, D. S.; Morgan, D. H. *J. Am. Chem. Soc.* **2005**, *127*, 10723.

(6) Agapie, T.; Labinger, J. A.; Bercaw, J. E. *J. Am. Chem. Soc.* **2007**, *129*, 14281.

(7) Emrich, R.; Heinemann, O.; Jolly, P. W.; Krueger, C.; Verhovnik, G. P. *J. Organometallics* **1997**, *16*, 1511.

(8) van Rensburg, W. J.; van den Berg, J.-A.; Steyner, P. *J. Organometallics* **2007**, *26*, 1000.

(9) Jabri, A.; Crewdson, P.; Gambarotta, S.; Kokobkov, I.; Duchateau, R. *Organometallics* **2006**, *25*, 715.

(10) McGuinness, D. S.; Brown, D. B.; Tooze, R. P.; Hess, F. M.; Dixon, J. T.; Slawin, A. M. Z. *Organometallics* **2006**, *25*, 3605.

(11) Agapie, T.; Schofer, S. J.; Labinger, J. A.; Bercaw, J. E. *J. Am. Chem. Soc.* **2004**, *126*, 1304.

(12) Tomov, A. K.; Chirinos, J. J.; Jones, D. J.; Long, R. J.; Gibson, V. C. *J. Am. Chem. Soc.* **2005**, *127*, 10166.

(13) Rucklidge, A. J.; McGuinness, D. S.; Tooze, R. P.; Slawin, A. M. Z.; Pelletier, J. D. A.; Hanton, M. J.; Webb, P. B. *Organometallics* **2007**, *26*, 2782.

stage of activation. Thus, chromium(III) ethylhexanoate, $\text{Cr}^{3+}(\text{EH})_3$, is proposed to be activated through one-electron inner shell reduction to $(\text{EH})_2\text{Cr}^{2+}$ initiated by AlEt_3 and accompanied by formation of ethyl radicals.¹⁵ Depending on the initial state of reduction, either a $\text{Cr}^{2+}/\text{Cr}^{4+}$ ^{9,10,15} or a $\text{Cr}^+/\text{Cr}^{3+}$ redox couple^{5,11,13,16} is assumed, and this is also dictated by the nature of the backbone ligand. Most of the mechanistic studies have been dedicated to ethylene trimerization so far. For this reaction, assumptions on the valence state of the active Cr redox couple have been generally based on comparisons of the catalytic performance when using defined precursor complexes with known Cr valence states synthesized ex situ and disregarding the fact that the Cr valence in the truly active site may differ from that in the precursor. To date there have been few experimental studies to investigate the mechanistic details of selective ethylene tetramerization and the redox chemistry involved. It is the objective of this work to obtain authentic information on the various steps of catalyst formation and activation from precursor states as well as on the behavior of the active complex during Cr-catalyzed ethylene oligomerization. Therefore, we have for the first time monitored the evolution of the $\text{Cr}(\text{acac})_3/\text{PNP}/\text{MMAO}$ catalytic system from precursor components as well as its interaction with ethylene at elevated temperature and pressure by in situ EPR spectroscopy, which provides direct access to different Cr valence states. For comparison, a preformed $[(\text{PNP})\text{CrCl}_2(\mu\text{-Cl})_2]$ complex containing two trivalent Cr sites was also investigated.

Experimental Section

(*i*-Pr)PPh₂ was prepared as described elsewhere.² MMAO-3A with 7 wt % Al in heptane was obtained from Akzo Nobel. The $[(\text{PNP})\text{CrCl}_2(\mu\text{-Cl})_2]$ complex was prepared as described elsewhere.^{2,17} All manipulations were performed in the absence of moisture and air in a glovebox, and predried solvents have been used.

EPR spectra were recorded on an ELEXSYS 500-10/12 cw-spectrometer (Bruker) with a microwave power of 6.3 mW, a modulation frequency of 100 kHz, and a modulation amplitude of 0.1, 0.3, or 0.5 mT. The magnetic field was measured with reference to the standard 2,2-diphenyl-1-picrylhydrazyl hydrate (DPPH). Spectra at 77 K were recorded in liquid N₂ using a finger dewar. Measurements at elevated temperature and under 10 bar of ethylene were performed in a thick-wall quartz tube (inner diameter: 3 mm) implemented into a variable-temperature control unit (Bruker) and connected by a Swagelok fitting to the ethylene bottle. Computer simulation of Cr^{3+} EPR spectra was performed with the program SIM14S of Lozos et al.¹⁸ using the spin Hamiltonian (eq 1) in which μ_B is the Bohr magneton, S is the electron spin operator, g is the g tensor, B_0 is the magnetic field vector, A is the hyperfine coupling tensor, and I is the nuclear spin operator.

$$H = \mu_B S g B_0 + S A I \quad (1)$$

The concentration of Cr^{3+} in selected samples was determined by comparing the EPR signal areas (double integrals) of Cr^{3+} with that of a 2.6×10^{-4} M solution of DPPH in heptane. For these measurements, a rectangular double cavity (Bruker) was used. The

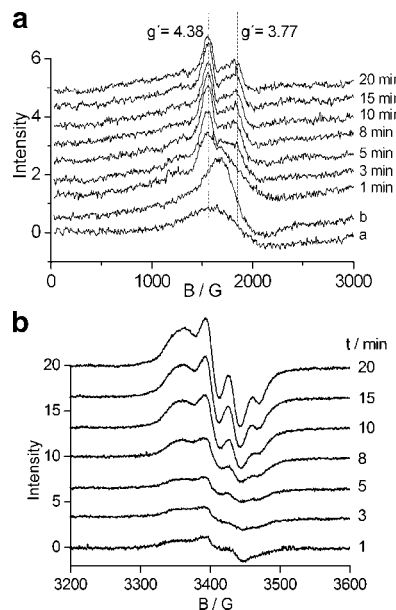


Figure 1. EPR spectra measured at 77 K of Cr-ac (a), Cr-ac/PNP (b), and Cr-ac/PNP/MMAO after 1, 3, 5, 8, 10, 15, and 20 min storage at room temperature. In case a and b no signals were observed in the range between 3200 and 3600 G (bottom plot).

concentration of the DPPH standard solution was determined photometrically.

Dry cyclohexane solutions of 1.0 mmol L^{-1} $\text{Cr}(\text{acac})_3$ (Cr-ac) or 1.0 mmol L^{-1} $\text{Cr}(\text{acac})_3 + 1.0 \text{ mmol L}^{-1}$ PNP (Cr-ac/PNP) were prepared in a glovebox. Then $200 \mu\text{L}$ of these solutions was added to $50 \mu\text{L}$ of MMAO–heptane solution in the EPR tube under dry argon by a syringe just before recording the spectra.

The same procedure was followed with the dimer complex $[(\text{PNP})\text{CrCl}_2(\mu\text{-Cl})_2]$, which was dissolved in dried toluene to result in a solution containing 1.0 mmol L^{-1} Cr, being equal to the one maintained for Cr-ac/PNP in cyclohexane.

Results and Discussion

In Situ Formation and Stability of the Cr Complex from $\text{Cr}(\text{acac})_3$ and PNP in the Absence of Ethylene. The EPR spectra of Cr-ac and Cr-ac/PNP show no signals at room temperature, probably due to short relaxation times. At 77 K, Cr-ac shows a signal at an effective g value of $g' \approx 4.3$ (Figure 1a), which arises from isolated Cr^{3+} species in a distorted geometry¹⁹ (Scheme 1, species **1a**).

The position of the signal is in agreement with previous studies in which it has been shown that this distortion arises from the ligand field with D_3 symmetry and comes from the dipole moments associated with the carbonyl groups of the acac ligands.²⁰ Upon adding the PNP ligand, the signal becomes more asymmetric, suggesting a superposition of two lines with similar position but different line widths (Figure 1a, spectrum b). This may be a consequence of the partial replacement of acac by PNP. Given that PNP is a neutral bidentate ligand, it could be assumed that the superimposed signal is due to an $[(\text{acac})_{3-y}\text{Cr}(\text{PNP})_y]^{3+}$ cation in which Cr^{3+} retains its oxidation state. Then the replaced acac[−] should act as a counterion. This case is visualized in Scheme 1 (species **1b**), which accounts also for the hypothetical coordination of more than one PNP ligand per Cr ion. Alternatively, it may be assumed that acac

(14) Chen, E. Y.-X.; Marks, T. J. *Chem. Rev.* **2000**, *100*, 1391.

(15) van Rensburg, W. J.; Grove, C.; Steynberg, J. P.; Stark, K. B.; Huyser, J. J.; Steynberg, P. J. *Organometallics* **2004**, *23*, 1207.

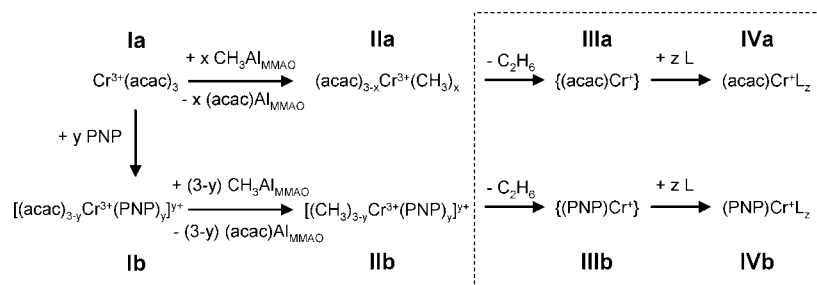
(16) Köhn, R. D.; Smith, D.; Mahon, M. F.; Prinz, M.; Mihan, S.; Kociok-Köhn, G. J. *Organomet. Chem.* **2003**, *683*, 200.

(17) McGuinness, D. S.; Wasserscheid, P.; Keim, W.; Hu, C.; Englert, U.; Dixon, J. T.; Grove, C. *Chem. Commun.* **2003**, 334.

(18) Lozos, G. P.; Hofman, B. M.; Franz, C. G. *Quantum Chemistry Programs Exchange* **1973**, 265.

(19) Weckhuysen, B. M.; De Ridder, L. M.; Grobet, P. J.; Schoonheydt, R. A. *J. Phys. Chem.* **1995**, *99*, 320.

(20) Singer, L. S. *J. Chem. Phys.* **1955**, *23*, 379.

Scheme 1. Possible Reaction of MMAO with Cr Complexes^a

^a Species in the dashed box are postulated as arising from species **IIa** and **IIb** for $x = 2$ and $y = 1$, respectively.

changes to monodentate bonding to allow the coordination of additional PNP. This would mean that species **Ib** in Scheme 1 reflects also complexes in which the denticity of acac is relaxed to allow weak interaction of PNP with the metal center. In any case, this would lead to changes in the Cr^{3+} coordination geometry, which agree with the fact that just the line shape changes but the total signal intensity around $g' \approx 4.3$ remains nearly unchanged upon adding PNP (compare Figure 1a, spectra a and b). Unfortunately, superhyperfine coupling between the Cr^{3+} electron spin and the ^{31}P nuclear spin ($I = 1/2$), which would be unequivocal evidence for coordination of the PNP ligand to Cr, is not resolved in the experimental spectrum of Figure 1 (top). Thus, the assignment of the respective EPR signal to a $[(\text{acac})_{3-y}\text{Cr}(\text{PNP})_y]^{y+}$ species (Scheme 1, **Ib**), though plausible, is an assumption.

As soon as MMAO is added to the Cr-ac/PNP solution, the total Cr^{3+} EPR intensity decreases gradually with the time that the mixture was kept at room temperature before quenching to 77 K (Figure 1, top). Moreover the splitting into two signals, reflecting two different remaining Cr^{3+} species, is more obvious from the low-field range in Figure 1. Taking account of the generally accepted opinion that aluminoxane activators alkylate the metal and abstract anions,^{1,8,14} it is assumed that the two different Cr^{3+} complexes giving rise to the signals in the low-field range (Figure 1, top) contain also methyl ligands instead of acac. They may be tentatively represented by species **IIa** and **IIb** in Scheme 1.

From the EPR spectra alone it is not possible to specify if only partial or complete replacement of acac by methyl groups occurs. However, recent DFT calculations of the reaction of PNPCrCl_3 complexes with MAO containing trimethyl aluminum (TMA) show a clear tendency for the replacement of all three Cl ligands by methyl groups, whereby the methylating aptitude of TMA was shown to be superior in relation to that of MAO.⁸ MMAO-3A used in this work is manufactured by controlled hydrolysis of a 70:30 mixture of TMA and triisobutyl aluminum (TIBA). Since the aluminoxane:alkyl aluminum molar ratio is typically 1.3:1, it is highly probable that MMAO-3A also contains residual TMA, which may favor complete over partial methylation and replacement of the acac ligands. In this case, species **IIa**, **IIIa**, and **IVa** in Scheme 1 would contain CH_3 instead of acac.

With the decline of the Cr^{3+} signals, a group of signals simultaneously arises in the field range between 3200 and 3600 G as the low-field signals around $g' \approx 4.3$ decrease (Figure 1, bottom). A signal in the same field range also appears when the $\text{Cr}(\text{acac})_3$ solution is mixed with MMAO in the absence of the PNP ligand (Figure 2B, solid line). Spectra simulation revealed that in the latter case the experimental line can be fitted by an axial signal with $g_{\parallel} = 2.0127$ and $g_{\perp} = 1.9868$ (Table 1,

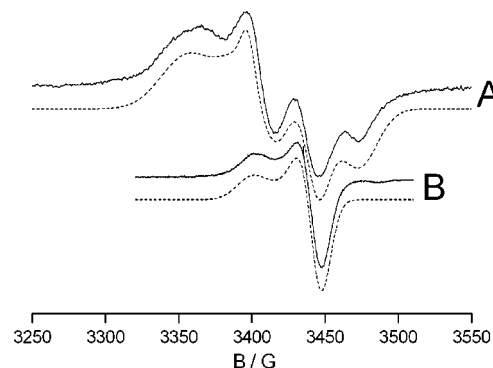


Figure 2. (A) EPR spectrum of Cr-ac/PNP/MMAO measured at 77 K after 20 min storage at room temperature (solid line, compare Figure 1, bottom) and calculated with the spin Hamiltonian parameters listed in Table 1 (dashed line); (B) same spectra for Cr-ac/MMAO in the absence of PNP after 1 min storage at room temperature.

Table 1. Spin Hamiltonian Parameters Obtained by Fitting the Cr^{3+} EPR Spectra Measured at 77 K after Storing Cr-ac/PNP/MMAO and Cr-ac/MMAO at Room Temperature (Figure 2)

	Cr-ac/PNP/MMAO				Cr-ac/MMAO	
	g_1	g_2	g_3	$I_{\text{rel}}/\%$	g_{\parallel}	g_{\perp}
species 1	2.0134	1.9875		57	2.0127	1.9868
species 2	2.0406	2.0099	1.9695	43		

Figure 2B dashed line). Signals with similar g tensor components have been observed from low-spin Cr^+ complexes (d^3 , $s = 1/2$) with different ligands in frozen solutions.^{21–23} Thus, this result shows clearly that Cr^{3+} is reduced to Cr^+ in the presence of MMAO, although the Cr^+ visible by EPR comprises only a small percentage of the total Cr content in the sample. This issue will be discussed in more detail below. Alkylation of the Cr^{3+} complexes alone should not change the Cr valence state. This requires a subsequent reduction process for which different possibilities can be discussed. For example, subsequent reduction could proceed via reductive elimination of two methyl groups forming ethane.

This is exemplified by the reactions within the dashed box in Scheme 1, for which it is assumed that in the respective parent species **IIa** and **IIb** $n = 2$ and $m = 1$. The resulting species **IIIa** and **IIIb** after reductive elimination of ethane are coordinatively unsaturated and should therefore be highly unstable.

(21) Farrell, I. R.; Hartl, F.; Zalis, S.; Wanner, M.; Kaim, W.; Vlcek, A., Jr *Inorg. Chim. Acta* **2001**, 318–143.

(22) Rieger, A. L.; Rieger, P. H. *Organometallics* **2002**, 21, 5868.

(23) Cummings, D. A.; McMaster, J.; Rieger, A. L.; Rieger, P. H. *Organometallics* **1997**, 16, 4362.

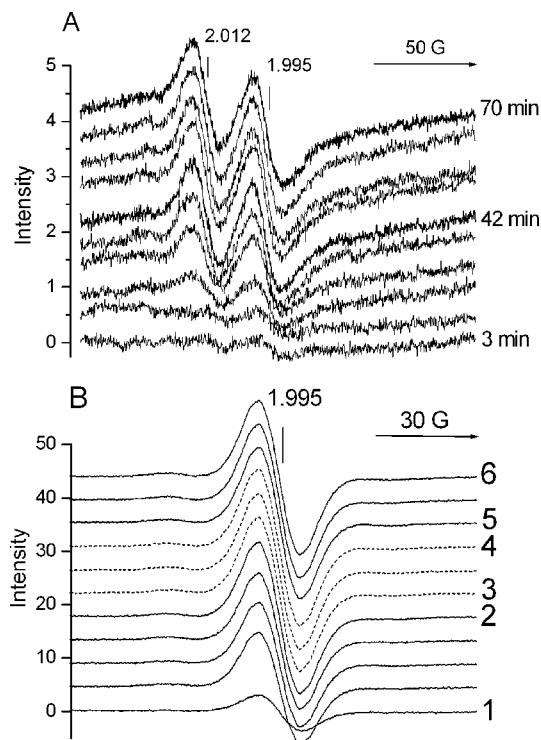


Figure 3. EPR spectra of (A) a Cr-ac/PNP/MMAO mixture measured at 313 K as a function of reaction time and (B) a Cr-ac/MMAO mixture measured as a function of temperature and time: (1) 313 K, 2 min; (2) 313 K, 60 min; (3) 323 K, 2 min; (4) 323 K, 15 min; (5) 333 K, 2 min; (6) 333 K, 30 min.

Most probably, unsaturation would be alleviated by coordination of additional ligands L, e.g., solvent molecules, further CrL_n , or MMAO units, to form stable species **IVa** and **IVb**, which are reflected by the EPR signals in Figure 2. Interestingly, the respective Cr^+ signal in the presence of PNP and MMAO can only be reproduced satisfactorily by superimposing two different Cr^+ sites, one of which shows axial symmetry similar to the one found for the Cr-ac/MMAO system without PNP and the other with rhombic symmetry characterized by three principle g tensor components at $g_1 = 2.0406$, $g_2 = 2.0099$, and $g_3 = 1.9695$ (Table 1, Figure 2A dashed line). The rhombic subsignal most probably arises from reduction of a PNP-containing Cr^{3+} complex (probably species **IIb** in Scheme 1), while the axial signal might form upon reduction of the respective PNP-free Cr^{3+} complex (species **IIa**, Scheme 1).

As mentioned above, the Cr^{3+} EPR signal in Figure 1a (spectrum b) before adding MMAO may represent a mixture of the two species **Ia** and **Ib** in Scheme 1, while the remaining Cr^{3+} signals recorded after different times upon contact with MMAO (Figure 1, top) could arise from the species **IIa** and **IIb**. Consequently, the reduced Cr^+ species in the bottom plot of Figure 1 should reflect species **IVa** and **IVb** on the right-hand side of Scheme 1. The same processes seem to occur at a higher rate when the temperature is increased. Thus, no Cr^{3+} EPR signal can be detected at 77 K when the Cr-ac/PNP/MMAO mixture is quenched after 15 min storage at 313 K. This might be due to complete reduction of Cr^{3+} under these conditions. When measured at higher temperature, the anisotropic g tensor splitting of the Cr^+ signals is lost (Figure 3).

This is due to the rapid tumbling of the Cr^+ species in solution, which averages out the g anisotropy. Consequently, two isotropic Cr^+ signals with g values of 2.012 and 1.995 are observed for the Cr-ac/PNP/MMAO system (Figure 3A), while

only one signal at $g_{\text{iso}} = 1.995$ arises in the absence of PNP (Figure 3B). An isotropic Cr^+ EPR signal was also observed from a solution of $\text{Cr}(\text{acac})_3$ and AlEt_3 in different aromatic solvents.²² For certain ligands coordinating via P atoms to Cr^+ , ^{31}P superhyperfine structure splitting of the EPR signal has been observed in previous studies.^{19–21} For the signals in Figures 1–3 this is, however, not the case. The P–Cr bond is probably too long to account for strong spin–spin interaction.

In principle, an EPR signal similar to that observed for low-spin Cr^+ can also be expected for a Cr^{5+} complex which shows the same total spin (d^1 , $S = 0.5$).^{23–25} However, in the latter case the g values were found to be considerably smaller than observed for low-spin Cr^+ , usually around 1.97 or lower. Thus, the signals arising upon contact with MMAO at g values around 2 (Table 1, Figures 1–3) can clearly be assigned to Cr^+ , which is evidence that the interaction of both the Cr-ac and Cr-ac/PNP catalyst precursor with the MMAO activator can lead to monovalent Cr^+ .

By comparing the EPR signals in Figure 3 it is evident that the Cr^+ signal amplitude arising after adding MMAO is higher in the absence of PNP. In this case, the signal of the reduced Cr^+ complex increased quickly during the first 15 min at 313 K and reaches its final intensity after 1 h contact with MMAO at 313 K (Figure 3B). Subsequent heating for 15 min at 323 K and 30 min at 333 K did not change the signal shape, suggesting that this Cr^+ complex is stable under these conditions. A similar behavior was also observed for the Cr-ac/PNP/MMAO system. However, the signal increase was slower than in the absence of the PNP ligand. At 313 K the maximum Cr^+ intensity was slowly reached only after 1 h. Further heating to 333 K (not shown) did not change the total intensity (Figure 3A). For precise quantitative evaluation, not the signal amplitude but the EPR signal area derived by double integration must be followed. This has been done for the Cr^{3+} signal at $g \approx 4.3$ (measured at 77 K) and the Cr^+ signal at $g \approx 2$ (measured at room temperature) in the systems Cr-ac/MMAO and Cr-ac/PNP/MMAO as a function of the time where the samples were kept at room temperature after adding MMAO. The Cr^+ concentrations have been derived by comparison of the EPR double integrals with those of the DPPH spin standard solution. As an example, the time dependence of the Cr^{3+} signal area and the Cr^+ concentration in the system Cr-ac/PNP/MMAO is plotted in Figure 4. The experimental values have been fitted by a pseudo-first-order rate law for the reduction of Cr^{3+} (eq 2) and the formation of Cr^+ (eq 3).

$$[\text{Cr}^{3+}] = [\text{Cr}^{3+}]_0 (e^{-kt}) \quad (2)$$

$$[\text{Cr}^+] = [\text{Cr}^{3+}]_0 (1 - e^{-kt}) \quad (3)$$

The fits are represented by the lines in Figure 4. The rate constants and relative EPR-visible Cr^+ concentrations are listed in Table 2.

Since the EPR signal in Cr-ac/PNP/MMAO is small and noisy in the initial period of reaction (Figure 3), double integration provides meaningful results only for the stronger signals at higher reaction times. For the same reason, double integrals of the Cr^{3+} signals for reaction times above 12 min could not be used.

As is evident from the obtained kinetic fits (Table 2), decline of the Cr^{3+} signal is much faster than formation of the Cr^+

(24) Angelescu, E.; Nicolau, C.; Simon, Z. *J. Am. Chem. Soc.* **1966**, *88*, 3910.

(25) Strassner, Th.; Muehlhofer, M.; Grasser, S. *J. Organomet. Chem.* **2002**, *641*, 121.

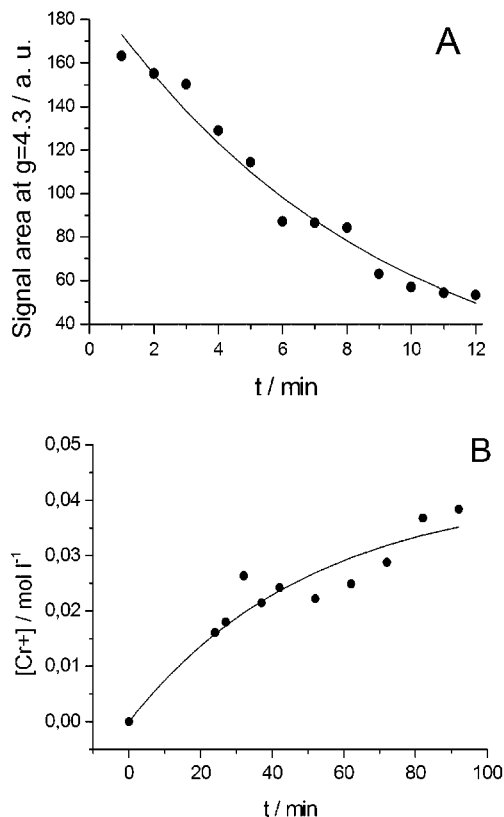


Figure 4. Evolution of the Cr^{3+} signal area (A) and the Cr^+ concentration (B) for the system Cr-ac/PNP/MMAO as a function of time after adding MMAO at room temperature. Lines represent fits according to a pseudo-first-order rate law.

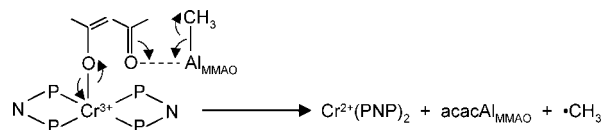
Table 2. Relative Cr^+ Concentrations Determined after 1 h and First-Order Rate Constants for the Decline of Cr^{3+} and the Formation of EPR-Active Cr^+

	$[\text{Cr}^+]/[\text{Cr}_{\text{total}}]/\%$	$k(\text{Cr}^{3+})/10^{-2}$ min^{-1}	$k(\text{Cr}^+)/10^{-2}$ min^{-1}
Cr-ac/MMAO	5.8	3.49 ± 0.34	10.12 ± 0.52
Cr-ac/PNP/MMAO	4.8	1.96 ± 0.64	11.36 ± 0.69

signal. Moreover, the EPR-visible Cr^+ concentrations reached after 1 h amount to $0.046 \text{ mmol l}^{-1}$ for Cr-ac/MMAO and to $0.038 \text{ mmol l}^{-1}$ for Cr-ac/PNP/MMAO. This corresponds to only 5.8% and 4.8%, respectively, of the total Cr amount in the samples. The mismatch between rate constants for Cr^{3+} and Cr^+ as well as the low Cr^+ concentration suggest that an EPR-silent Cr species is formed.

Two main possibilities can be proposed for the formation of such a species. One is (i) dimerization or even agglomeration of mononuclear Cr^+ complexes to form antiferromagnetically coupled $\text{Cr}^+ \cdots \text{Cr}^+$ dimers and/or clusters. In this case, spin pairing would lead to a loss of EPR intensity while the Cr^+ species retain their valence state. Dimer and/or cluster formation could occur as a consequence of reductive elimination of ethane, for example, to alleviate unsaturation of the transient species **IIIa** and **IIIb** (Scheme 1). The EPR signal at $g \approx 2$ should then arise from residual Cr^+ species that did not dimerize and/or are formed by cleavage of the dimers. The observed relation of Cr^{3+} depletion and Cr^+ formation rate would rather support the latter pathway. Both relative concentration and formation rate of Cr^+ are somewhat smaller when PNP is present in the solution. Possibly PNP may be better able to bridge two Cr^+ ions, thus supporting dimer formation.

Scheme 2. Proposed Mechanism for Direct Reduction of Cr^{3+} by MMAO in Analogy with Previous Suggestions¹⁵



(ii) Another reason could be that reduction of Cr^{3+} does not proceed to Cr^+ but stops already at Cr^{2+} , which is not detectable by EPR under the conditions applied. This should be more probable for the Cr-ac/PNP/MMAO system. Assuming elimination of methyl radical intermediates from species **IIIb** (Scheme 1) as the cause of reduction, this process should stop at Cr^{2+} when more than one PNP ligand is coordinating to the same Cr ion, thus leaving less than two CH_3 groups per Cr ion for reductive elimination. The same situation would arise when inner shell electron transfer, in analogy to the reduction of $\text{Cr}(\text{EH})_3$ by AlEt_3 ,¹⁵ is assumed as the reason for reduction (Scheme 2).

Considering the ratio of Cr:PNP = 1 as well as the fact that, in the presence of PNP, a PNP-free Cr^+ complex is still detected by EPR (Figure 3A, $g = 1.995$), it is straightforward to assume that Cr complexes with two PNP ligands may indeed be formed. To obtain more information on the relation between Cr^{3+} reduction and number of PNP ligands in the complex, the interaction of MMAO with solutions containing PNP:Cr ratios of 1, 2, and 3 has been studied at room temperature (Figure 5). It is clearly seen that the Cr^+ signal decreases markedly for PNP:Cr = 2 and vanishes completely for PNP:Cr = 3. This shows clearly that coordination of two or three PNP ligands to the same Cr site might suppress reduction to Cr^+ . However, it must also be mentioned that an attempt to detect methyl radical formation by performing the reaction in the presence of a spin trap (*N-tert-butyl- α -phenylnitron*) was not successful. Moreover, recent DFT calculations suggest that the most appropriate PNP-Cr intermediates present during methylation contain Cr in its trivalent form.⁸ Thus, the Cr valence state of the majority of the Cr species, the possibility of Cr site agglomeration, and the route of Cr^+ formation in the presence of MMAO is still uncertain. To obtain more clarity on these issues in the presence and absence of PNP, further studies by XAS and EPR at liquid helium temperature are planned that could visualize divalent Cr^{2+} .

Interaction of the Cr Complexes Formed in Situ from $\text{Cr}(\text{acac})_3$ and PNP with Ethylene. In previous studies it was found that tetramerization of ethylene with Cr-ac/PNP/MMAO is optimally performed at 333 K under 45 bar of ethylene

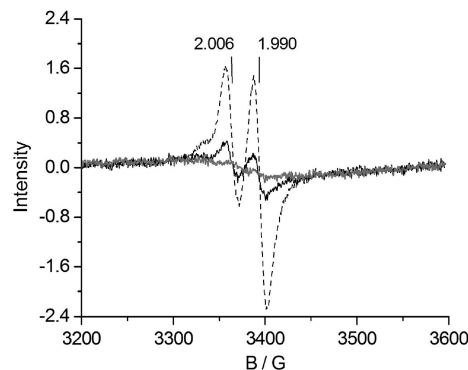


Figure 5. In situ EPR spectra of Cr-ac/PNP/MMAO with different PNP:Cr ratios measured 25 min after adding MMAO at room temperature: PNP:Cr = 1 (dashed line), PNP:Cr = 2 (solid black line), PNP:Cr = 3 (gray line).

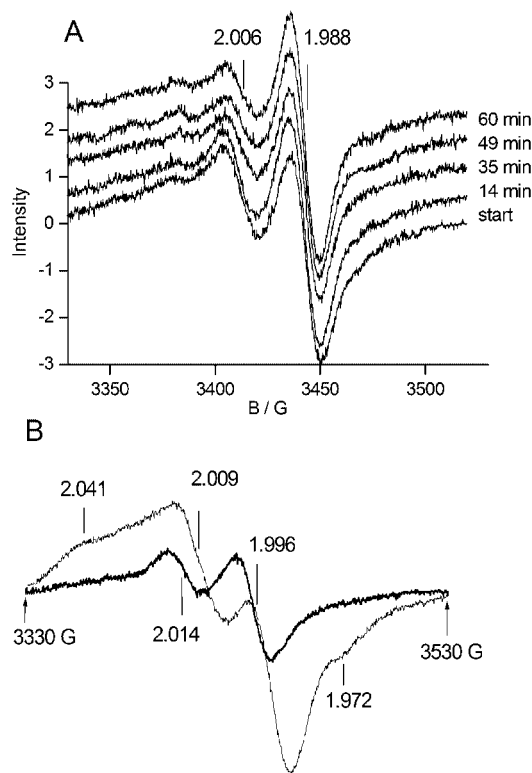


Figure 6. In situ EPR spectra of Cr-ac/PNP/MMAO (A) during isothermal treatment at 333 K with 10 bar of ethylene and (B) after the reaction at room temperature (thick line) and 77 K (thin line).

pressure in a stirred autoclave.⁵ For experimental reasons, only a pressure of 10 bar of ethylene could be applied in the in situ EPR experiment, and no stirring was possible. Immediately after mixing, the Cr-ac/PNP/MMAO solution was placed at 333 K in the EPR cavity, pressurized with 10 bar of ethylene, and spectra were recorded as a function of time (Figure 6A). It can be seen that the Cr⁺ signal at $g = 2.006$ (assigned tentatively to species **IVb** in Scheme 1) broadens slightly and decreases in amplitude, while the one at $g = 1.988$ (assigned tentatively to species **IVa** in Scheme 1) remains constant. Interestingly, the former signal recovers upon cooling, i.e., after the reaction has stopped. Both the isotropic and anisotropic features are well visible in the spectra of the quenched system at room temperature and 77 K (Figure 6B). This suggests that the intensity decrease observed under reaction conditions for Cr-ac/PNP/MMAO is transient in nature.

In any case, it is probable that the Cr⁺ EPR signals in Figure 6A do not comprise the major part of the active Cr species, since they represent only a minor part of the total Cr amount in the samples. Nevertheless, they do reflect the influence of ethylene in a different way. While the signal at $g = 1.988$ (assigned to Cr⁺ species not containing PNP) does not change, the one at $g = 2.006$ (assigned to Cr⁺ species containing PNP) broadens reversibly (Figure 6A). If one assumes that the catalytic activity is related to a working Cr⁺/Cr³⁺ redox cycle as postulated previously,^{5,9,11,13,16} for example, this redox cycle should periodically restore the EPR-active Cr⁺ state. The valence dynamics connected with this redox cycle might cause line broadening, leading to the observed temporal intensity loss of the Cr⁺ signal. Interestingly, this effect is not observed for the signal at $g_{\text{iso}} = 1.988$ assigned to a PNP-free Cr⁺ species (species **IVa** in Scheme 1). In agreement with previous catalytic

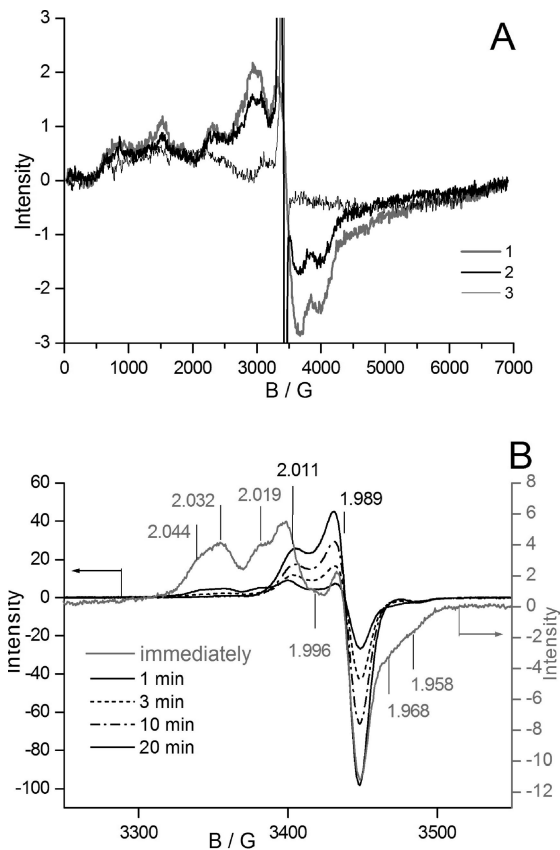


Figure 7. (A) EPR spectra measured at 77 K of the [(PNP)CrCl₂(μ -Cl)]₂ complex in toluene without MMAO (1), immediately after adding MMAO (2), and after 10 min storage at 293 K in the presence of MMAO (3). (B) Enlarged region of Figure 6A measured at 77 K after different times in contact with MMAO at 293 K.

test results, this suggests that the PNP-free Cr complex is less active in ethylene tetramerization.

Although the reversible change of the EPR signal of the PNP-containing Cr⁺ complex strongly suggests that such species are actively involved in a redox cycle when ethylene is present (Figure 6A), it must be recalled that they represent only a minor fraction of the total Cr in the sample. This suggests that the major active species might be EPR silent. Possibly, Cr⁺ dimers act as the resting state from which the active Cr⁺ species are temporarily formed by cleavage as discussed earlier.¹⁶ The above-mentioned fast redox cycle could then broaden the EPR signal beyond detection. Alternatively, divalent Cr²⁺ cannot be excluded as an active site.

Behavior of the Pre-prepared [PNP-*i*-Pr-CrCl₂(μ -Cl)]₂ Complex. The results described above have shown that identification of the particular structure of the active complex formed in situ in a solution containing Cr(acac)₃ and PNP is not straightforward. Therefore, the interaction of MMAO and ethylene with a separately synthesized [(PNP)CrCl₂(μ -Cl)]₂ complex of known structure has also been studied. Due to the poor solubility of this complex in cyclohexane, toluene has been used as the solvent. The EPR spectrum of the complex in toluene shows several signals distributed over a wide field range (gray line in Figure 7A). These signals originate most probably from fine structure splitting of a distorted Cr³⁺ site with a total electron spin of 3/2. Depending on the size of the fine structure parameters, which itself is determined by the local symmetry of the Cr³⁺ site, the EPR transitions can give rise to several

signals.²⁶ A detailed assignment would be possible only by spectra simulation.

The influence of time on the interaction of MMAO with the $[(\text{PNP})\text{CrCl}_2(\mu\text{-Cl})_2]$ complex is evident from Figure 6B. Spectra were measured at 77 K after storing the mixtures with MMAO for different times at room temperature. For each spectrum a fresh sample was mixed. After adding the complex/toluene solution to MMAO and immediate cooling to 77 K, the Cr^{3+} signal decreases slightly (thick black line in Figure 7A) and a new narrow signal characteristic of Cr^+ appears in the spectrum (gray line in Figure 7B). With increasing storage time at 293 K, the Cr^{3+} signals disappear (thin black line in Figure 7A) and the Cr^+ line increases strongly (Figure 7B), suggesting fast reduction of Cr^{3+} to Cr^+ under these conditions.

Detailed inspection of the narrow field range in which the Cr^+ appears (Figure 7B) shows a single axial Cr^+ signal growing with storage time at room temperature with g tensor components at $g_{\parallel} = 2.011$ and $g_{\perp} = 1.989$ (Figure 7B), which are very similar to the parameters of the Cr^+ site formed upon contact of $\text{Cr}(\text{acac})_3$ with MMAO (Figure 2B, Table 1). When the sample is quenched immediately after contact of the complex with MMAO, at least two further anisotropic Cr^+ lines are visible (gray line in Figure 7B), which disappeared, however, after 3 min storage at 293 K before quenching to 77 K. This suggests that the complex undergoes fast structural changes in the initial period of interaction with MMAO, which may lead to its degradation.

By comparison of Figure 7B and Figure 1B it is readily evident that the intensity of the Cr^+ signal is much larger in the former case, suggesting that either reduction of Cr^{3+} to Cr^+ in the presence of MMAO is markedly more pronounced and/or the formation of antiferromagnetic dimers is suppressed for the $[(\text{PNP})\text{CrCl}_2(\mu\text{-Cl})_2]$ complex compared to Cr-ac/PNP/MMAO .

When the EPR spectra of the $[(\text{PNP})\text{CrCl}_2(\mu\text{-Cl})_2]/\text{MMAO}/\text{toluene}$ solutions (Figure 8A) are measured after warming to room temperature, the anisotropy of the g tensor is lost due to rapid tumbling of the Cr^+ species in solution. Instead, a very characteristic isotropic, superhyperfine structure multiplet is observed (Figure 8A).

This superhyperfine structure arises from the coupling of the electron spin of Cr^+ ($S = 1/2$) with the nuclear spins ($I = 1/2$) of 10 equivalent protons (from two toluene molecules). This coupling must give rise to a multiplet with 11 superhyperfine lines and an intensity distribution of 1:10:45:120:210:252:210:120:45:10:1. With the exception of the outer two lines, which might be too weak, all of these lines are observed and can be made even more visible when plotting the second derivative of the spectrum (Figure 8B). The isotropic values $g_{\text{iso}} = 1.988$ and $A_{\text{iso}} = 3.57$ G as well as the hyperfine coupling constant of the electron spin ($S = 1/2$) with the nuclear spin of the ^{53}Cr isotope ($I = 3/2$, natural abundance 9.5%; $A(^{53}\text{Cr}) = 18$ G) are in excellent agreement with values found for the $[\text{Cr}(\eta^6\text{-CH}_3\text{C}_6\text{H}_5)_2]^+$ cation in CH_3CN solution.²⁷ The same Cr^+ sandwich complex was also detected upon reaction of $\text{Cr}(\text{acac})_3$ with AlEt_3 in toluene solution.²² In this case electroneutrality of the solution was maintained by formation of AlEt_4^- anions.

The complex $[(\text{PNP})\text{CrCl}_2(\mu\text{-Cl})_2]$ is only a catalyst precursor, which must be transformed into the active Cr species upon

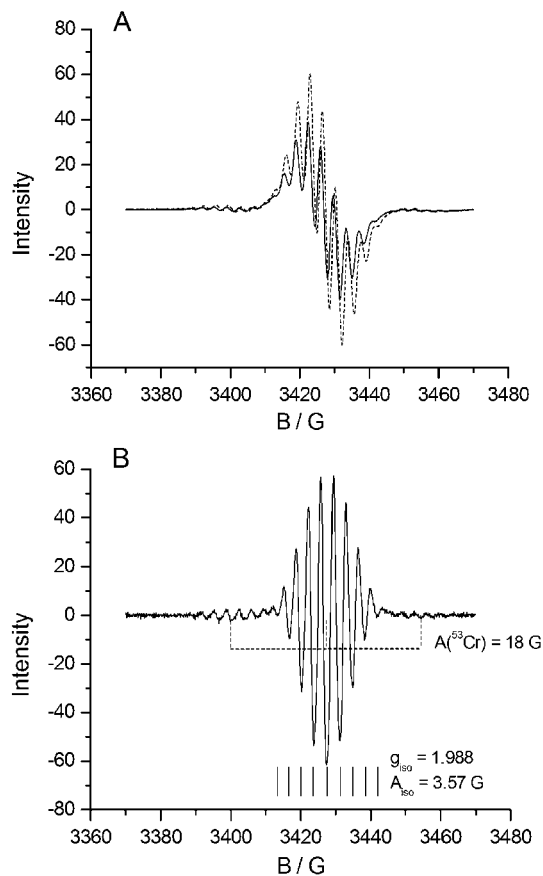


Figure 8. (A) EPR spectra of $[(\text{PNP})\text{CrCl}_2(\mu\text{-Cl})_2]$ in toluene measured at 293 K after 5 min (solid line) and 15 min (dashed line) contact with MMAO and (B) second derivative of the spectrum after 15 min.

contact with MMAO. However, the identification of the $[\text{Cr}(\eta^6\text{-CH}_3\text{C}_6\text{H}_5)_2]^+$ cation is clear evidence that this transformation occurs alongside the undesired release of the PNP ligand. Probably the same processes as proposed in Scheme 1 for Cr-ac/MMAO take place upon contact with MMAO, namely, methylation followed by reductive elimination. The resulting vacant coordination sites are then saturated by toluene, which is even able to displace the PNP ligand. The much higher EPR Cr^+ intensity in comparison to the Cr-ac/PNP/MMAO system might be due to the fact that sandwiching by two toluene molecules prevents agglomeration and the formation of EPR-silent Cr^+ species.

In Figure 9 EPR spectra are plotted during interaction of the complex/MMAO mixture with 10 bar of ethylene.

During the first hour at 313 K, no change of shape and intensity was observed. Therefore, the reaction temperature was raised to 323 K. Figure 9 shows the last EPR spectrum after 60 min at 313 K together with spectra recorded after 5, 15, and 30 min at 323 K and after raising the temperature again to 333 K. It can be seen clearly that the intensity of the signal originating from the $[\text{Cr}(\eta^6\text{-CH}_3\text{C}_6\text{H}_5)_2]^+$ cation increases during reaction at 323 K and further at 333 K. This suggests that the undesired release of the PNP ligand is even more pronounced under these conditions, which might be a consequence of the higher temperature. Previous catalytic tests revealed that this catalyst in toluene solution shows lower reaction rates in comparison to the Cr-ac/PNP/MMAO system in cyclohexane. As evidenced by the EPR results, this might be due to the rapid decomposition of the active complex.

(26) Brückner, A. In *Spectroscopy of Transition Metal Ions on Surfaces*; Weckhuysen, B. M.; Van Der Voort, P., Catana, G., Eds.; Leuven University Press: Leuven, 2000; p 69.

(27) Weeks, C. L.; Levina, A.; Dillon, C. T.; Turner, P.; Fenton, R. R.; Lay, P. A. *Inorg. Chem.* **2004**, *43*, 7844.

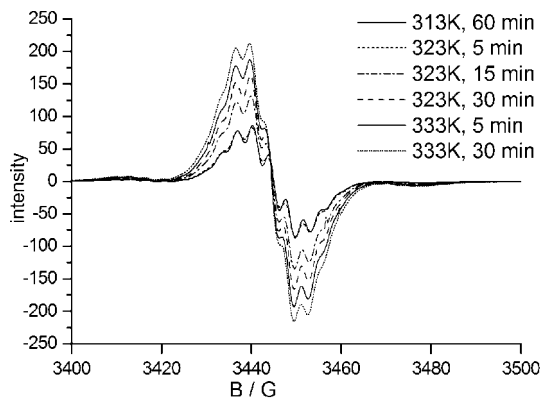


Figure 9. Evolution of EPR spectra during reaction of [(PNP)CrCl₂(μ-Cl)]₂/MMAO with ethylene.

Conclusions

The results show clearly that Cr³⁺ in the initial Cr-ac/cyclohexane, Cr-ac/PNP/cyclohexane, and [PNP-*i*-Pr-CrCl₂(μ-Cl)]₂/toluene solutions is reduced to low-spin Cr⁺ in the presence of MMAO. However, the amount of EPR-visible Cr⁺ differs strongly in the order Cr-ac/PNP < Cr-ac ≪ [(PNP)CrCl₂(μ-Cl)]₂, although the total Cr concentration in the three solutions was the same. The low percentage of EPR-visible Cr⁺ in the Cr-ac and Cr-ac/PNP solutions might be due to antiferromagnetically coupled Cr⁺•••Cr⁺ dimers and/or clusters that are built from unsaturated Cr intermediates formed as a consequence of reduction. However, particularly in the case of Cr-ac/PNP, reduction to EPR-silent Cr²⁺ cannot be excluded. In the case of [(PNP)CrCl₂(μ-Cl)]₂ much more Cr⁺ is visible by EPR, since the active Cr species formed from this precursor complex releases the PNP ligand and is embedded between two toluene ligands, which might prevent agglomeration.

In the Cr-ac/MMAO solution, one Cr⁺ species with axial symmetry is detected by EPR, while in the Cr-ac/PNP/MMAO system a second Cr⁺ species with rhombic symmetry is observed. The latter is attributed to a Cr⁺ complex that contains a coordinated PNP ligand. Since the solution contains a ratio of Cr: PNP = 1 and a PNP-free Cr⁺ complex is still visible by EPR, it is possible that also Cr complexes with two PNP ligands are formed, which, however, might

be reduced to EPR-silent Cr²⁺. This conclusion is supported by the fact that the Cr⁺ intensity is strongly reduced for ratios of PNP:Cr ≥ 1 (Figure 5).

Interaction of ethylene with Cr-ac/PNP/MMAO leads to a transient broadening of the EPR signal tentatively assigned to the PNP-containing Cr⁺ complex, which is only evident under reaction conditions and which is not observed for the signal assigned to the PNP-free Cr⁺ complex. This broadening could be related to fluctuation of the Cr valence state between +1 and +3 due to a redox cycle and can be considered as a hint for the active participation of this Cr⁺ species in the catalytic reaction. However, since this Cr⁺ complex comprises only a minor amount of the total Cr content in the solution, the presence of a further active but EPR-invisible Cr species is highly probable. This could be a transient Cr⁺ species that is formed from an antiferromagnetic Cr⁺ dimer resting state but is not detectable due to line broadening caused by the redox cycle operating during reaction.

In contrast to the in situ-formed Cr complex in cyclohexane solution, the [(PNP)CrCl₂(μ-Cl)]₂ catalyst precursor is transformed into [Cr(η⁶-CH₃C₆H₅)₂]⁺ cations with a sandwich structure in the presence of MMAO. This means that the complex loses the PNP ligand. This destruction is even more severe at reaction temperature and can obviously not be prevented in the presence of ethylene. Despite the same total Cr concentration, formation of EPR-visible Cr⁺ in the [(PNP)CrCl₂(μ-Cl)]₂/MMAO/ethylene system is more pronounced by about 2 orders of magnitude than for the system Cr-ac/PNP/MMAO/ethylene (compare Figures 6A and 9). This may be due to the fact that agglomeration to antiferromagnetic Cr⁺ dimers and/or clusters is suppressed due to sandwiching by two toluene ligands. The previous observation of reduced reaction rates in toluene indicates that this solvent might not be suitable for ethylene tetramerization since the catalytically active Cr complex is destroyed.

Acknowledgment. We thank Sasol Technology UK Ltd. and Sasol Technology (Pty) Ltd. for financial support and permission to publish as well as Dr. D. H. Morgan Dr. J. T. Dixon for valuable discussions.

OM800316M